Biogeosciences

Impacts of climate and reclamation on temporal variations in CH$_4$ emissions from different wetlands in China: from 1950 to 2010

T. Li[1], W. Zhang[1], Q. Zhang[1], Y. Lu[2], G. Wang[1], Z. Niu[3], M. Raivonen[4], and T. Vesala[4,5]

[1]LAPC, Institute of Atmospheric Physics, Chinese Academy of Sciences, Beijing 100029, China
[2]Anhui Climate Center, Hefei 230031, China
[3]State Key Laboratory of Remote Sensing Science, Jointly Sponsored by Institute of Remote Sensing Applications, Chinese Academy of Sciences and Beijing Normal University, Beijing 100101, China
[4]Department of Physics, P.O. Box 48, 00014 University of Helsinki, Finland
[5]Department of Forest Sciences, P.O. Box 27, 00014 University of Helsinki, Finland

Correspondence to: W. Zhang (zhw@mail.iap.ac.cn)

Abstract. Natural wetlands are among the most important sources of atmospheric methane and thus important for better understanding the long-term temporal variations in the atmospheric methane concentration. During the last 60 years, wetlands have experienced extensive conversion and impacts from climate warming which might result in complicated temporal and spatial variations in the changes of the wetland methane emissions. In this paper, we present a modeling framework, integrating CH4MOD$_{wetland}$, TOPMODEL, and TEM models, to analyze the temporal and spatial variations in CH$_4$ emissions from natural wetlands (including inland marshes/swamps, coastal wetlands, lakes, and rivers) in China. Our analysis revealed a total increase of 25.5 %, averaging 0.52 g m^{-2} per decade, in the national CH$_4$ fluxes from 1950 to 2010, which was mainly induced by climate warming. Larger CH$_4$ flux increases occurred in northeastern, northern, and northwestern China, where there have been higher temperature rises. However, decreases in precipitation due to climate warming offset the increment of CH$_4$ fluxes in these regions. The CH$_4$ fluxes from the wetland on the Qinghai–Tibet Plateau exhibited the lowest CH$_4$ increase (0.17 g m^{-2} per decade). Although climate warming has accelerated CH$_4$ fluxes, the total amount of national CH$_4$ emissions decreased by approximately 2.35 Tg (1.91–2.81 Tg), i.e., from 4.50 Tg in the early 1950s to 2.15 Tg in the late 2000s, due to the wetland loss totalling 17.0 million ha. Of this reduction, 0.26 Tg (0.24–0.28 Tg) was derived from lakes and rivers, 0.16 Tg (0.13–0.20 Tg) from coastal wetlands, and 1.92 Tg (1.54–2.33 Tg) from inland wetlands. Spatially, northeastern China contributed the most to the total reduction, with a loss of 1.68 Tg. The wetland CH$_4$ emissions reduced by more than half in most regions in China except for the Qinghai–Tibet Plateau, where the CH$_4$ decrease was only 23.3 %.

1 Introduction

Atmospheric methane (CH$_4$) is the second-most important trace greenhouse gas (GHG) after carbon dioxide (CO$_2$). In IPCC (2013), the radiative forcing of CH$_4$ was revised to 0.97 W m^{-2} when its indirect global warming effect was incorporated. The atmospheric CH$_4$ concentration has increased by ∼ 150 % from 1750 to 2011 (IPCC, 2013) but remained nearly constant from 1999 to 2006 and then continually increased after 2007 (Nisbet et al., 2014). However, the temporal variation in the inventory-based estimates of methane emissions exhibited a different trend. Human-derived CH$_4$ emissions substantially increased (10 %) from 2000 to 2005 due to rapid economic growth and increasing demand for food and energy, implying inaccuracies in the inventories, simultaneously offsetting the decreases in natural emissions or a comparable increase in atmospheric CH$_4$ removals such as the OH radical (Montzka et al., 2011).

Natural wetland emissions are the largest natural source as well as the most uncertain source in the global CH$_4$ bud-

get (Denman et al., 2007; Potter et al., 2006; Whalen, 2005), ranging from 115 (Fung et al., 1991) to 237 Tg CH$_4$ yr^{-1} (Hein et al., 1997) , and representing 20 to 40 % of the global source. However, it has been reported that the long-term loss of natural wetlands was approximately 50 % during the 20th century (Moser et al., 1996; Revenga et al., 2000), and as high as 87 % since 1700 (Davidson, 2014). Additionally, the wetland loss may have offset the increase in human-derived CH$_4$ emissions from 2000 to 2005 (Bousquet et al., 2006).

China has the world's fourth largest wetland area (z. Wang et al., 2012) and contains a wide variety of representative types of the world's natural wetlands. The Chinese natural wetlands have also experienced a serious loss, with 23 % in freshwater swamps, 16 % in lakes, 15 % in rivers, and 51 % in the coastal wetlands during the past 60 years based on census data (An et al., 2007), attributed primarily to reclamation (An et al., 2007; Niu et al., 2012; Huang et al., 2010; Xu and Tian, 2012). Analysis with the remote sensing data also reported that ∼ 30 % of the wetlands were lost during the past 30 years (Niu et al., 2012). Accounting for reclamation in the national CH$_4$ estimates is important because it has inevitably reduced CH$_4$ emissions.

Most studies estimating the national CH$_4$ emissions from natural wetlands have involved the extrapolation of site-specifically measured methane fluxes (Wang et al., 1993; Khalil et al., 1993; Jin et al., 1999; Ding et al., 2004; Ding and Cai, 2007; Chen et al., 2013; X. K. Wang et al., 2012). Induced by the substantial heterogeneity in wetland CH$_4$ fluxes (e.g., Christensen et al., 2003; Ding et al., 2004; Yang et al., 2006) and the disagreement in data of the wetland area (e.g., Zhao and Liu, 1995; Xu et al., 1995; X. K. Wang et al., 2012; Zhao, 1999), there are large uncertainties in the national wetland CH$_4$ emission inventories of 4.4 (1.7–10.5) Tg CH$_4$ yr^{-1}. In addition, the measured fluxes may also yield biased estimations when temporally extrapolated to the distant past, such as the 1950s, when no experiment data were available. The process-based models are capable of reducing the bias by quantifying the impacts of environmental changes on wetland methane emissions in the modeling mechanism. A few modeling studies have simulated the national CH$_4$ emissions from the inland marshes/swamps of China (Xu and Tian, 2012; Tian et al., 2011). However, lakes, rivers, and coastal wetlands are also non-negligible in estimating national CH$_4$ budget and the temporal trend (Bastviken et al., 2004; Yang et al., 2011; Chen et al., 2013). To date, there has been no comprehensive study on national CH$_4$ emissions from all kinds of natural wetlands in China from 1950 to 2010.

To make an estimation of the national CH$_4$ fluxes for the last 60 years, reproducing the time series of the national wetland area back to 1950 is necessary. Recently, Niu et al. (2012) developed maps of the natural wetlands (including inland marshes/swamps, lakes, rivers, and coastal wetlands) in 1978, 1990, 2000, and 2008, respectively. In addition, a biogeophysical model validated against the CH$_4$ flux mea-
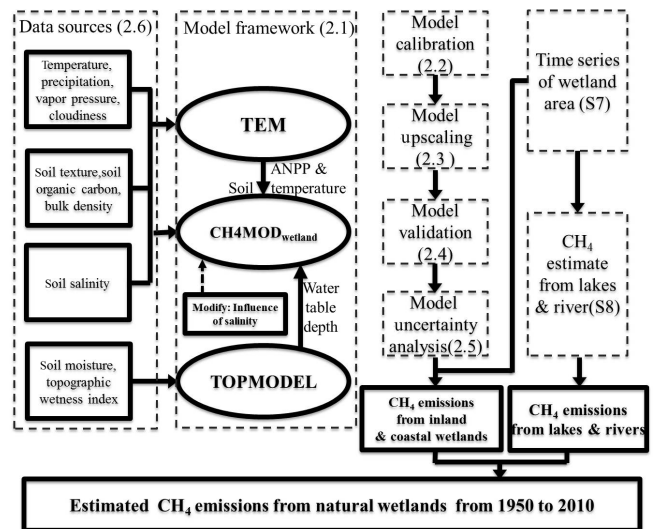

Figure 1. Framework of simulating CH$_4$ emissions from natural wetlands between 1950 and 2010 in China. CH4MOD$_{wetland}$ is a biogeophysical model to simulate CH$_4$ fluxes from natural wetlands. TEM is a process-based biogeochemistry model that couples carbon, nitrogen, water, and heat processes in terrestrial ecosystems to simulate ecosystem carbon and nitrogen dynamics. TOPMODEL is a conceptual rainfall–runoff model that is designed to work at the scale of large watersheds using the statistics of topography.

surements representative of the wetlands around the world, i.e., CH4MOD$_{wetland}$ (Li et al., 2010), facilitates the long-term modeling of the methane emissions from all types of the natural wetlands in China. Thus the objectives of the present study are (1) to model spatial and temporal changes in CH$_4$ emissions across China's natural wetlands (including inland marshes/swamps, lakes, rivers, and coastal wetlands) from 1950 to 2010 and (2) to quantify the impacts of climate change and reclamation on the CH$_4$ emissions from the natural wetlands in different regions of China.

2　Materials and methods

In this study, we used an integrated modeling framework centered on CH4MOD$_{wetland}$ (Li et al., 2010) to simulate the CH$_4$ emissions from inland and coastal wetlands. Directly extrapolated field measurements were used to calculate the CH$_4$ emissions from lakes and rivers (Chen et al., 2013). A diagram in Fig. 1 shows the main steps of the methods for estimating the national CH$_4$ emissions from the natural wetlands from 1950 to 2010.

2.1　Modeling framework

Three models were included in the model framework with a spatial resolution of 0.5° for the period from 1950 to 2010 (Fig. 1). The center of the modeling framework is CH4MOD$_{wetland}$ (Li et al., 2010). CH4MOD$_{wetland}$ is a bio-

geophysical model that aims to simulate the CH$_4$ production, oxidation, and emissions from natural wetlands (Li et al., 2010). In CH4MOD$_{wetland}$, methane production rates are calculated by the availability of methanogenic substrates and the parameterized influences of environmental factors, e.g., soil temperature, soil texture, and soil redox potential. The methanogenic substrates are derived from the root exudation of wetland plants and the decomposition of above- and belowground litters and the soil organic matter. The CH$_4$ emissions to the atmosphere via diffusion, ebullition, and plant transportation are all simulated in the model. Oxidation occurs when CH$_4$ diffuses to the atmosphere or is transported via the plant aerenchyma.

The model inputs include the soil texture (soil sand fraction, soil organic carbon, and bulk density), aboveground net primary productivity (ANPP), daily soil temperature, water table depth, and salinity. With the modeling outputs of the daily CH$_4$ emissions (g m^{-2} d^{-1}), we multiplied the CH$_4$ fluxes by the wetland area in each $0.5° \times 0.5°$ grid and summed the CH$_4$ emissions from all grids to yield the total national CH$_4$ emissions (Fig. 1).

The validation of CH4MOD$_{wetland}$ against the field measurements of CH$_4$ fluxes from wetlands across China, Canada, and the USA presents details of the model performance (Li et al., 2010, 2012). At present, however, the insufficiency of the model mechanism, e.g., lacking the influence of thawing permafrost on CH$_4$ production, will result in distorted CH$_4$ simulations during the winter and freeze–thaw period. The dynamics of the water table and the growth of wetland plants also limit its upscaling to regions where no measurements of the water tables and ANPP are available. Therefore, we integrated two other models, i.e., TEM and TOPMODEL, to facilitate upscaling of CH4MOD$_{wetland}$.

The TEM model (Melillo et al., 1993; Zhuang et al., 2004, 2006, 2007, 2013) is a process-based biogeochemistry model that couples carbon, nitrogen, water, and heat processes in terrestrial ecosystems to simulate ecosystem carbon and nitrogen dynamics. This model has been widely used to investigate regional and global NPP (e.g., Melillo et al., 1993; Cramer et al., 1999; McGuire et al., 1992). With this model framework (Fig. 1), the soil temperature and net primary productivity (NPP) outputs from the TEM model were used as inputs to CH4MOD$_{wetland}$. The fraction of ANPP to NPP was determined based on Gill and Jackson (2003). Further descriptions of the model and the inputs are described in Zhuang et al. (2013).

TOPMODEL (Beven and Kirby, 1979) is a rainfall–runoff model that is designed to work at the scale of large watersheds using the statistics of topography. In previous research (Bohn et al., 2007; Kleinen et al., 2012; Lu and Zhuang et al., 2012; Zhu et al., 2013), TOPMODEL has been used to simulate water table variations in natural wetlands. The TOPMODEL inputs included soil moisture and the topographic wetness index (Fig. 1). More details on simulating water table depth using TOPMODEL are provided in Supplement S1.

Previous studies (Atkinson and Hall, 1976; King and Wiebe, 1978; Bartlett et al., 1985, 1987; Magenheimer et al., 1996) have indicated that methane emissions from various coastal salt marshes in the temperate zone vary with salinity. To improve the capacity to simulate methane emissions from coastal wetlands, we adopted the relationship between salinity and methane fluxes according to Poffenbarger et al. (2011):

$$f(s) = 10^{a \times s}, \tag{1}$$

where $f(s)$ represents the effect of salinity on CH$_4$ production, s is the salinity (psu, practical salinity unit), and a is an empirical constant.

2.2 Model calibration

The natural wetlands in China have complex plant species. Considerable spatial variations in fluxes related to vegetation have been found (Ding et al., 2004; Hirota et al., 2004; Song et al., 2007; Duan et al., 2005; Huang et al., 2005). Such variations have been ascribed mainly to the differences in the plant NPP, the capacity of transferring labile organic carbon into anoxic environments, and the capacity for the plant transport and oxidation of CH$_4$ (Berrittella and Huissteden, 2011). Sufficient calibration and parameterization of the vegetation parameters in the model is important for reliably reproducing CH$_4$ emissions at wetland sites. *Carex* and *Phragmites* are dominant plant species in Chinese natural wetlands (Lang and Zu, 1983). Previous site measurements (Table S1 in the Supplement) on the wetlands with *Carex* and *Phragmites* provide the data for model calibration and validation.

In the present study, the recalibrated parameters of CH4MOD$_{wetland}$ are mainly related to the vegetation (Table S2). Among these parameters, the proportion of the roots to the total production (f_{root}) and the fraction of available plant-mediated transport (T_{veg}) were obtained from the literature. VI is a vegetation index that can identify the relative differences in methane production among vegetation types, and P_{ox} recognizes the different fractions of CH$_4$ oxidized when transported by different plant species. Both VI and P_{ox} were calibrated to account for the differences between plant species.

In our previous studies, we parameterized VI and P_{ox} using the CH$_4$ flux measurements collected from the Sanjiang Plain (SJ site in Table S1) in Region I (Fig. 2), where the dominant plant species is *Carex* (Supplement S3, Li et al., 2010, 2012). In this study, we used the minimum RMSE method to recalibrate VI and P_{ox} for the wetlands dominated by *Phragmites* (Table S2). More details about the calibration and minimum RMSE method can be found in Supplement S2. Table S2 shows the values and sources of the model parameters.
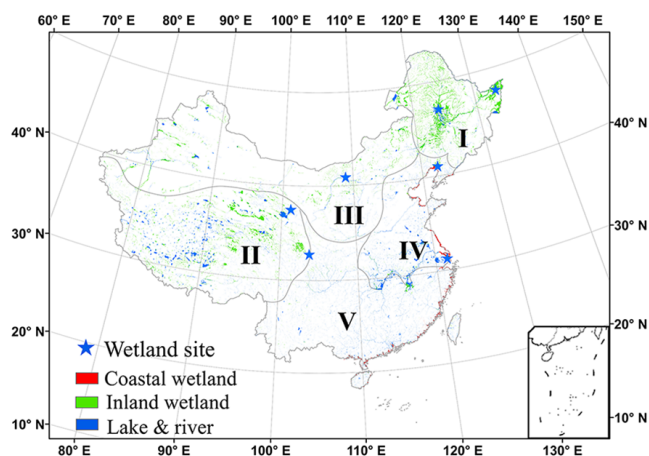
Figure 2. Wetland regions across China. The blue stars are the locations of the wetland sites. The wetland distribution map is from the remote sensing data in 1978.

2.3 Upscaling of the model framework

Lang and Zu (1983) divided the Chinese wetlands into five regions according to the environmental conditions and dominant vegetation type (Fig. 2). Supplement S3 describes details about the climate, soil, and vegetation type of the regions. For national model simulations of CH$_4$ fluxes, we adopted this spatial partition and assigned the vegetation-related parameters of CH4MOD$_{wetland}$ with the calibrated values in Table S2 to each division. Upscaling of the model parameters is explained in Supplement S4.

We established gridded ($0.5° \times 0.5°$) and geo-referenced time-series input data sets of climate, soil, and salinity data to drive the modeling in each grid (Fig. 1). The total CH$_4$ emission from the inland and coastal wetlands in each grid cell was calculated as the product of the CH$_4$ fluxes and the gridded wetland area.

2.4 Model validation

Model validation evaluates the model performance at the "site scale" using individual CH4MOD$_{wetland}$ simulations and at the "grid scale" using the proposed model framework (Fig. 1). More details regarding the site-scale and the grid-scale validations are described in Supplement S5.

The site-scale validations were carried out at the wetland sites on the Sanjiang Plain (Fig. S1a, b in the Supplement), the Ruoergai Plateau (REG in Table S1; Fig. S1d, e), the Haibei alpine marsh (HB in Table S1; Fig. S1g), the Zhalong wetland (ZL in Table S1; Fig. S1i), and the Liao River delta (LRD in Table S1; Fig. S1k). The comparison of the simulated versus the observed monthly CH$_4$ fluxes resulted in an R^2 of 0.79, with a slope of 0.86 and an intercept of 0.73 ($n = 41$, $p < 0.001$; Fig. S2a). The RMSE, mean deviation (RMD), and the model efficiency (EF) between the sim-

ulated and observed monthly CH$_4$ fluxes were 48.5, 0.9, and 0.78 %, respectively.

The grid-scale validation showed that the integrated model framework (CH4MOD$_{wetland}$/TEM/TOPMODEL, Fig. 1) was able to simulate the seasonal variations in monthly CH$_4$ emissions at SJ (Fig. S1c) and LRD (Fig. S1l). Though there are some underestimations in the CH$_4$ fluxes predicted by the model framework for the other three sites (Fig. S1f, h, and j), the measured monthly CH$_4$ fluxes fell in or near the range of the modeled CH$_4$ emissions (Fig. S2b). For the grid-scale validation, the regression of simulated versus observed monthly CH$_4$ emissions resulted in an R^2 of 0.79, with a slope of 0.84 and an intercept of -0.11 ($n = 41$, $p < 0.001$). The RMSE, RMD, and EF between the simulated and observed monthly CH$_4$ fluxes were 51.3, -17.8, and 0.75 %, respectively, for the integrated model framework.

2.5 Uncertainty analysis

Uncertainty in the estimated regional CH$_4$ emissions from natural wetlands may originate from many sources. The Monte Carlo method has been widely used in uncertainty analysis. However, the Monte Carlo method is computationally expensive. In this study we focused on the uncertainties induced by the inputs of ANPP, the water table depth, and the soil sand fraction, using the extreme condition approach (Du and Chen, 2000; Li et al., 1996, 2004, 2012; Giltrap et al., 2010; Kesik et al., 2005). The comparison of these two methods is in Supplement S6. We designed eight extreme scenarios with a cross combination of the maximum and minimum values of ANPP, water table depth, and the soil sand fraction, ± 10 % from their baseline values. The simulated minimum and maximum CH$_4$ fluxes of the eight scenarios were considered representative of the modeling uncertainty range. For more details of the estimate under the baseline and scenarios, please see Supplement S6.

2.6 Data sources

The data sources include site-specific observations for model calibration and validation, the gridded input data sets for driving model framework as well as the wetland area. Table S1 provides detailed site descriptions. The CH$_4$ emissions were measured weekly or monthly at these sites. Most of the sites have synchronous measurements of the climate and water table depth. Figure 2 shows the locations of the sites.

The gridded input data sets are related with the climate, soil, vegetation, and the hydrology. We summarize the sources of the data sets in Table 1.

The gridded wetland maps of 1950, 1978, 1990, 2000, and 2008 were used in the regional modeling. The gridded wetland maps for 1978, 1990, 2000, and 2008 were obtained from Niu et al. (2012). The initial gridded wetland map of 1950 was estimated based on the remote sensing data of 1978 (Niu et al., 2012) and the census data (An et al., 2007). Sup-

Table 1. Summary of the gridded input data sets for driving the model framework.

	Gridded input data sets	Sources
Climate	Air temperature[5,2] Precipitation[5,2] Vapor pressure[5,2] Cloudiness[5,2]	The Climatic Research Unit (CRU TS 3.10) of the University of East Anglia in the United Kingdom (Harris et al., 2014)
Soil	Soil texture[1,2] Soil organic carbon[1] Soil bulk density[1] Soil salinity[5,1] Soil moisture[5,3] Soil temperature[5,7,2]	Food and Agriculture Organization (FAO, 2012) Harmonized World Soil Database (HWSD; FAO, 2008) World Ocean Atlas 2009 (Antonov et al., 2010) Fan and van den Dool (2004) Outputs of TEM (this study)
Hydrology	Topographic wetness index[3] Water table depth[5,7,1]	HYDRO1k Elevation Derivative Database (USGS, 2000) Outputs of TOPMODEL (this study)
Vegetation	Vegetation map[4] ANPP[6,1] Plant phenology[6,1]	DISCover Database (Belward et al., 1999; Loveland et al., 2000) Outputs of TEM (this study) Outputs of TEM (this study)

[1] Driving CH4MODwetland. [2] Driving TEM. [3] Driving TOPMODEL. [4] Specifies the vegetation parameters for CH4MOD$_{wetland}$ and TEM. [5] Monthly data from 1950 to 2010. [6] Annual data from 1950 to 2010. [7] We used the linear interpolation to develop the daily data sets.

plement S8 describes more details about the way of obtaining the time series of the wetland area.

3 Results

3.1 Spatiotemporal variations in CH$_4$ fluxes in China

The temporal change in CH$_4$ fluxes (CH$_4$ emissions per wetland area) were primarily driven by climate changes. In this section, we analyzed the seasonal and interannual variations in CH$_4$ fluxes from the inland and coastal wetlands from 1950 to 2010.

Figure 3 shows the seasonal variations in the modeled average CH$_4$ fluxes from 1950s to 2010s. A consistent pattern of the CH$_4$ flux peak occurred at the end of July across all regions and decades (Fig. 3). CH$_4$ fluxes were very low in January and February, especially in northern China and in the Qinghai–Tibet Plateau (Fig. 3a, b, and c), when the soil froze. In the warmer regions, such as Region V, CH$_4$ fluxes were much greater (Fig. 3e). The highest intra-annual flux variability was in northeastern and southern China (ca. 6.35–7.37 mg m^{-2} h^{-1}; Fig. 3a and e), with the Qinghai–Tibet Plateau showing the lowest variability (1.72–1.98 mg m^{-2} h^{-1}, Fig. 3b). Temporally, the highest intra-annual variability was in the 2000s for all regions, with 1970s and 1960s showing the lowest (Fig. 3).

Figure 4f provides the interannual variations and trends in the national annual CH$_4$ fluxes in China. The national annual CH$_4$ fluxes have significantly increased over the last 60 years, especially since 1980s. The national annual

CH$_4$ flux was 16.9 g m^{-2} yr^{-1} in 1950 and increased to 21.2 g m^{-2} yr^{-1} in 2010, with the average rate of 0.52 g m^{-2} per decade and a total increase of 26 % during the period from 1950 to 2010. The annual CH$_4$ fluxes fluctuated between 16.0 and 19.0 g m^{-2} yr^{-1} before 1980 and then increased rapidly in the 1990s. The highest annual CH$_4$ flux (22.5 g m^{-2} yr^{-1}) occurred in 1998, whereas the lowest (15.7 g m^{-2} yr^{-1}) occurred in 1954.

The estimated annual CH$_4$ fluxes in different regions are illustrated in Fig. 4. The highest CH$_4$ fluxes occurred in the northeastern (Fig. 4a, Region I) and southern (Fig. 4e, Region V) regions (24.8 and 20.0 g m^{-2} yr^{-1}, respectively), with the Qinghai–Tibet Plateau (Fig. 4b, Region II) showing the lowest (6.2 g m^{-2} yr^{-1}) and the other regions (e.g., Region III and IV) showing intermediate results (e.g., 8.8 and 13.5 g m^{-2} yr^{-1}, respectively; Fig. 4c and d).

Figure 4 also provides the trends in the annual CH$_4$ fluxes in different regions. There are significant increases ($p < 0.001$) in Regions I, II, III, and V (Fig. 4). The greatest increase in CH$_4$ fluxes occurred in Region I and Region V (0.67 and 0.54 g m^{-2} per decade, respectively; Fig. 4a and e), with Region II showing the lowest (0.17 g m^{-2} per decade, Fig. 4b) increase rate and Region III and Region IV showing an intermediate increase rate (0.42 and 0.52 g m^{-2} per decade, respectively; Fig. 4c and d).

3.2 Climate and CH$_4$ fluxes

Figure 5 presents the regional responses of CH$_4$ fluxes to temperature and precipitation. The simulated CH$_4$ fluxes in-
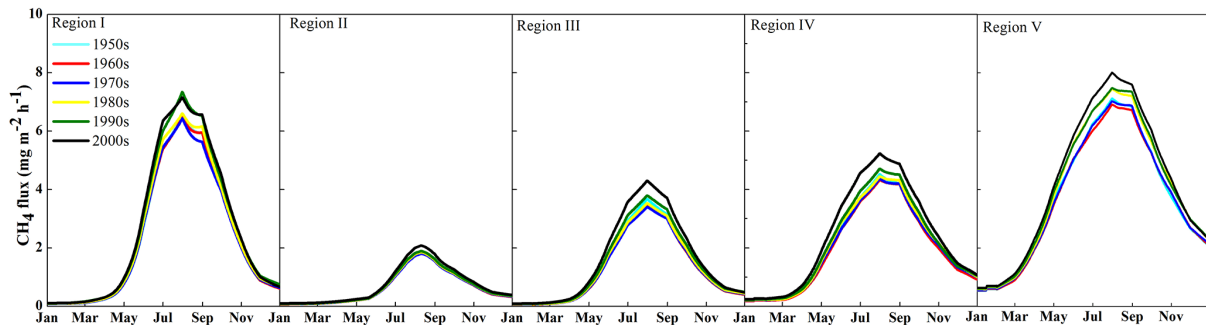
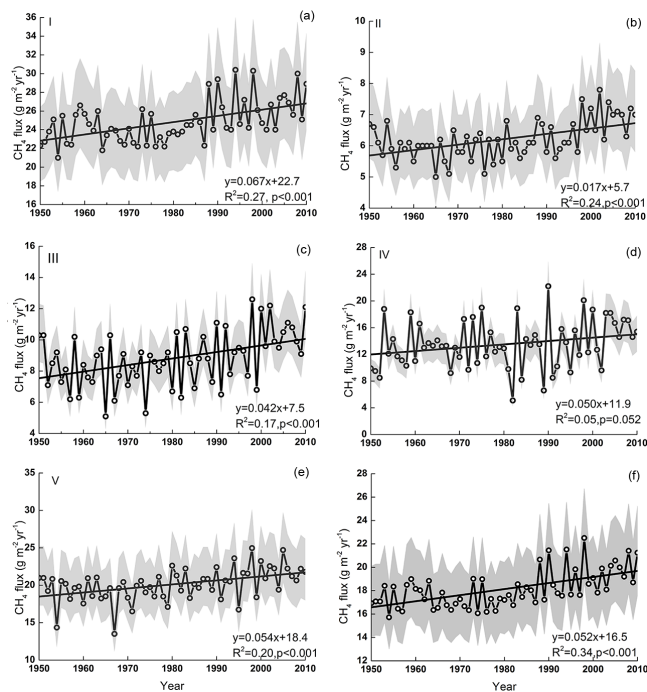**Figure 3.** Seasonal variations in methane fluxes in the five regions.

Figure 4. Methane fluxes from inland and coastal wetlands between 1950 and 2010 in **(a)** Region I, **(b)** Region II, **(c)** Region III, **(d)** Region IV, **(e)** Region V, and **(f)** all of China.

creased by ∼ 12 %, as a result of the air temperature increase of ∼ 1.35 °C during the past 60 years (Fig. 4f). The modeled 5-year CH$_4$ fluxes exhibited linear trends that closely follow the trends in air temperature in Region I (Fig. 5a), Region II (Fig. 5b), Region III (Fig. 5c), and Region V (Fig. 5e). The contribution of precipitation to the trends in CH$_4$ fluxes differed among the regions. During the past 60 years, Region I and Region III have experienced temperature increases by 0.29 °C per decade and 0.34 °C per decade, respectively. The warming trend resulted in CH$_4$ fluxes increasing by 0.67 g m^{-2} per decade (Fig. 4a) and 0.42 g m^{-2} per decade, respectively (Fig. 4c). In Region I, the CH$_4$ fluxes were predominantly positively correlated with air tempera-

ture ($R^2 = 0.35$, $p < 0.001$; Fig. 5a). Although no correlation was found between the CH$_4$ fluxes and the precipitation in Region I, the linear precipitation decrease of 38.3 mm per decade ($p < 0.001$) may have offset the increase in CH$_4$ fluxes due to the air temperature (Fig. 5a) before 1980. The linear precipitation decrease of 1.7 mm per decade ($p = 0.4$, not significant) in Region III may also have a negative impact on CH$_4$ fluxes (Fig. 5c). CH$_4$ fluxes in Region II showed a positive correlation with both temperature and precipitation (Fig. 5b). A slight temperature increase of 0.19 °C per decade and precipitation increase of 6.7 mm per decade resulted in a flux increase of 0.17 g m^{-2} per decade. In Region V, the positive correlation between CH$_4$ fluxes and temperature was more significant than with precipitation (Fig. 5e), suggesting that the temperature was the dominant factor in the acceleration of CH$_4$ fluxes during the past 60 years. The increase in the precipitation, at a rate of 16.6 mm per decade, though not significant ($p = 0.24$), may have benefited the CH$_4$ fluxes in this region. In Region IV, CH$_4$ fluxes were less responsive to temperature than precipitation (Fig. 5d). The increase in temperature also promoted CH$_4$ fluxes to increase at a rate of 0.50 g m^{-2} per decade (Fig. 4d).

Interannual or interdecadal variations in CH$_4$ fluxes were found to be closely aligned with variations in precipitation (Fig. 5). The lowest CH$_4$ fluxes usually accompanied periods of low precipitation. For example, the lowest CH$_4$ fluxes and precipitation occurred simultaneously during the period 1980–1985 in Region IV (Fig. 5d) and the period 1965–1970 in Region V (Fig. 5e). In Region I, the 5-year average CH$_4$ fluxes showed a trend that was synchronous with the 5-year average precipitation trend (Fig. 5a), decreasing before 1980 and then increasing until 1995. In Region I and Region II, there was excessive amounts of precipitation in the 1990s (Fig. 5a) and 2000s (Fig. 5b) in conjunction with the relatively high air temperatures, which resulted in the highest CH$_4$ fluxes. In contrast, when the greatest amount of precipitation occurred (Fig. 5c: from 1955 to 1960 in Region III; Fig. 5d: from 1960 to 1975 in Region IV; and Fig. 5e: from 1970 to 1975 in Region V), the CH$_4$ fluxes remained low due to the lower air temperatures. The linear regression (not shown) suggested that the CH$_4$ fluxes of 1950–
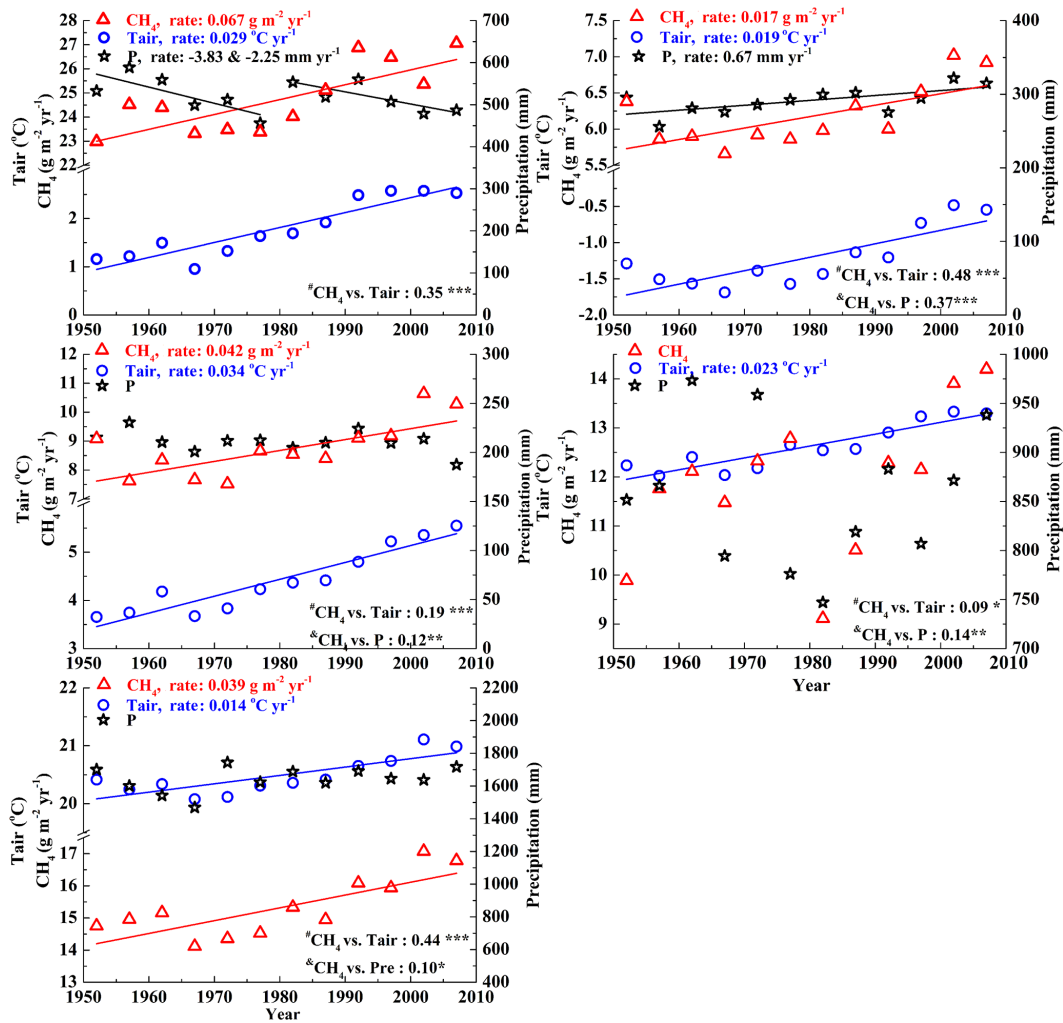
Figure 5. Impact of the climate factors on CH$_4$ fluxes from 1950 to 2010 in **(a)** Region I, **(b)** Region II, **(c)** Region III, **(d)** Region IV, and **(e)** Region V. The red triangles, blue circles, and the black stars are 5-year average CH$_4$ fluxes (the same data as in Fig. 4), air temperature, and precipitation, respectively. The slope represents the significant linear rate ($p < 0.05$). CH$_4$ vs. Tair: the correlation coefficient between the annual mean CH$_4$ fluxes and air temperature. CH$_4$ vs. P: the correlation coefficient between the annual mean CH$_4$ fluxes and the precipitation. Only correlations with statistical significance are shown ($p < 0.05$).

2010 increased $1.7\,\mathrm{g\,m^{-2}\,yr^{-1}}$ per 100 mm of precipitation ($R = 0.35$; $p < 0.05$) from the inland and coastal wetlands in China.

3.3 Changes in natural wetland area

The total wetland area in China was approximately 35.6 million ha in 1950 (Table 2). Our results show that there had been 17.0 million ha of wetland loss from 1950 to 2010, mostly during the first 50 years when the wetland areas decreased by 16.1 million ha. Since 2000, wetland loss has been limited (Table 2).

A large wetland loss of 7.8 million ha occurred in Region I, accounting for approximately 45.7 % of the total wetland loss of the nation (Table 2). Compared with 1950, the wetland areas decreased by 56.9, 24.6, 48.4, 65.3, and 46.7 % in Region I, Region II, Region III, Region IV, and Region V (Table 2), respectively.

Among the wetland types, the inland wetlands experienced the largest part of the area loss, with 10.3 million ha from 1950 to 2010, accounting for 60.6 % of the total wetland loss. More than 95 % of the inland wetland loss occurred in Region I, Region II, and Region III (Table 2). In contrast, coastal wetland loss occurred primarily in eastern and southern China (Region IV and Region V in Table 2). The coastal wetland losses were 68.5 % in 2008 compared to the area in 1950. The total area loss was 4.94 million ha for lake and river wetlands between 1950 and 2008. Substantial loss of lakes/rivers occurred in eastern China (Region IV).

Table 2. Regional CH_4 emissions and the wetland area.

		Region CH_4 emissions[1] (Tg)						Area[2] (M ha)					
		I	II	III	IV	V	China	I	II	III	IV	V	China
Inland wetland	1950	2.80	0.31	0.25	0.06	0.11	3.53	12.26	4.78	2.66	0.30	0.27	20.27
	1980	2.06	0.27	0.22	0.06	0.10	2.71	9.71	4.61	2.57	0.29	0.26	17.44
	1990	1.90	0.23	0.14	0.09	0.08	2.44	7.73	3.42	1.77	0.44	0.18	13.54
	2000	1.13	0.23	0.13	0.05	0.07	1.61	5.40	3.43	1.41	0.23	0.15	10.62
	2010	1.16	0.22	0.12	0.05	0.06	1.61	5.09	3.20	1.36	0.20	0.13	9.98
	Decrease[3]	−58.6 %	−29.0 %	−50.40 %	−16.7 %	−45.5 %	−54.4 %	−58.2 %	−33.3 %	−48.1 %	−33.3 %	−66.7 %	−50.8 %
Coastal wetland	1950	–	–	–	0.09	0.18	0.27	–	–	–	1.52	1.02	2.54
	1980	–	–	–	0.08	0.09	0.17	–	–	–	0.78	0.53	1.31
	1990	–	–	–	0.05	0.07	0.12	–	–	–	0.75	0.4	1.15
	2000	–	–	–	0.05	0.06	0.11	–	–	–	0.54	0.37	0.91
	2010	–	–	–	0.06	0.04	0.10	–	–	–	0.53	0.27	0.80
	Decrease[3]	–	–	–	−33.3 %	−77.8 %	−62.9 %	–	–	–	−65.1 %	−73.5 %	−68.5 %
Lakes and rivers	1950	0.08	0.29	0.08	0.22	0.04	0.70	1.38	5.19	1.49	4.05	0.68	12.79
	1980	0.07	0.26	0.07	0.20	0.03	0.62	1.20	4.62	1.27	3.55	0.56	11.21
	1990	0.05	0.22	0.04	0.13	0.03	0.47	0.91	3.83	0.78	2.32	0.51	8.35
	2000	0.04	0.22	0.04	0.11	0.03	0.45	0.76	3.87	0.77	1.93	0.61	7.94
	2010	0.04	0.25	0.04	0.07	0.04	0.44	0.79	4.32	0.78	1.31	0.65	7.85
	Decrease[3]	−50.0 %	−13.8 %	−50.0 %	−68.2 %	0.0 %	−37.1 %	−42.8 %	−16.8 %	−47.7 %	−67.7 %	−4.4 %	−38.6 %
Total wetland	1950	2.88	0.60	0.33	0.37	0.33	4.50	13.64	9.97	4.15	5.87	1.97	35.60
	1980	2.13	0.53	0.29	0.34	0.22	3.50	10.91	9.23	3.84	4.62	1.35	29.96
	1990	1.95	0.45	0.18	0.27	0.18	3.03	8.64	7.25	2.55	3.51	1.09	23.04
	2000	1.17	0.45	0.17	0.21	0.16	2.17	6.16	7.3	2.18	2.7	1.13	19.47
	2010	1.20	0.47	0.16	0.18	0.14	2.15	5.88	7.52	2.14	2.04	1.05	18.63
	Decrease[3]	−58.3 %	−23.3 %	−51.5 %	−51.4 %	−57.6 %	−52.2 %	−56.9 %	−24.6 %	−48.4 %	−65.3 %	−46.7 %	−47.7 %

[1] The average CH_4 fluxes of three consecutive years (including 1950–1952, 1979–1981, 1989–1991, 1999–2001, and 2008–2010) were used to calculated regional CH_4 emissions. For example, regional CH_4 emissions in 1980 were the production of the area of 1980 and the average CH_4 fluxes from 1979 to 1981. [2] Data of 1980, 1990, 2000, and 2010 were from the remote sensing data (Niu et al., 2012). The areas of 1978 and 2008 were regarded as the areas of 1980 and 2010, respectively. [3] Decrease means the reduce fraction in 2010 compared with 1950. "–": little or no wetland.

3.4 Changes in the regional CH_4 emissions due to climate change and wetland loss

Along with the wetland loss, our results show that the CH_4 emissions decreased by approximately 2.35 Tg (1.91–2.81 Tg) in China's wetlands, i.e., from 4.50 Tg in the early 1950s to 2.15 Tg in the late 2000s (Table 2), contrasting with the averaged increase in the CH_4 fluxes of 3.43 g m^{-2} due to climate changes (Fig. 4f). More than 99 % of the CH_4 reduction occurred before 2000 (Table 2).

The wetlands in Region I were the greatest contributor to the decreased CH_4 emissions, due to their holding the largest wetland area losses (Table 2) but also having the largest CH_4 flux increase due to climate warming and wetting, which, however, did not compensate for the CH_4 decrease from 1950 to 2010 (Fig. 2b). In Region I, the CH_4 emissions decreased by 58.3 % in the late 2000s compared with the early 1950s, with an aggregated loss of 1.68 Tg (1.36–2.03 Tg, Table 2). In other regions, the reduction in CH_4 emissions was 0.13–0.19 Tg, with a loss fraction of 23.3–57.6 % (Table 2). Among the regions, the lowest CH_4 reduction occurred in Region II, where only a slight loss in wetlands occurred. The loss of CH_4 emissions was 23.3 %, which is comparable to the wetland loss (Table 2).

Among the wetland types, the methane emissions decreased by 54.4, 62.9, and 37.1 % from inland wetlands, coastal wetlands and lakes/rivers, respectively (Table 2). Region I was the most important contributor to the decreased CH_4 emissions, which contributed 85.4 % to the regional CH_4 reduction for inland wetlands (Table 2). For the coastal wetlands, the substantial CH_4 reduction occurred in Region V, where CH_4 fluxes decreased by $\sim$ 82 %. The loss of coastal wetland was larger in Region IV than in Region V, but fluxes were 2.4 times larger in Region V, favoring its larger CH_4 emissions decrease.

4 Discussion

4.1 Regional estimates of CH_4 emissions in Chinese wetland

China has the world's fourth largest wetland area (Z. Wang et al., 2012) and contributes 4.4 (1.7–10.5) Tg CH_4 yr^{-1} to the atmosphere (Khalil et al., 1993; Jin et al., 1999; Ding et al., 2004; Ding and Cai, 2007; Chen et al., 2013; Wang et al., 1993; X. K. Wang et al., 2012). On a national scale, this amount is comparable to coal-bed emissions (5.45 Tg CH_4 yr^{-1}), residential biofuel combustion (2.28 Tg CH_4 yr^{-1}), landfills (4.35 Tg CH_4 yr^{-1}), biomass burning (1.6 Tg CH_4 yr^{-1}; Streets et al., 2001), emissions from rice cultivation ($\sim$ 8 Tg CH_4 yr^{-1}; Yan et al., 2009; Li et al., 2006a; Chen et al., 2013; Zhang et al., 2011), and emissions from livestock (8.55 Tg yr^{-1} Tg CH_4 yr^{-1}; Streets et al., 2001). Our model resulted in 2.17–3.03 Tg of the national CH_4 emissions from wetlands with an area of 19.5–23

M ha during the same period. In addition, the present study suggested that the substantial CH$_4$ emissions reduction simulated by CH4MOD$_{wetland}$ between 1950 and 2000 (2.35 Tg CH$_4$) was, however, half compensated for by the increase in paddy rice CH$_4$ emission over the same period (1.2 Tg in Zhang et al., 2011). In this study, the net greenhouse effect is not yet well understood. Because when the wetland was reclaimed to the upland, there were more N$_2$O emissions, which was not considered in this study.

Previous studies have estimated the national wetland CH$_4$ emissions by simply extrapolating the field measurements of CH$_4$ fluxes to the national scale (Wang et al., 1993, X. K. Wang et al., 2012; Khalil et al., 1993; Jin et al., 1999; Ding et al., 2004; Chen et al., 2013; Cai, 2012). The estimations of both Ding et al. (2004) and Chen et al. (2013) were primarily based on measurements from Ruoergai at the eastern edge of the Tibetan Plateau. Chen et al. (2013) used an observation of CH$_4$ fluxes that was much higher than the observation of Ding et al. (2004) during the 2000s, resulting in substantially higher emissions estimates from the wetlands of the Tibetan Plateau (Table 3). Moreover, the spatial characteristics show that Ruoergai has a higher CH$_4$ flux (Fig. 3) than other places on the Qinghai–Tibet Plateau, e.g., Huashixia (5.3–6.7 g m^{-2} yr^{-1}) with an altitude of 4000 m in the central Qinghai–Tibet Plateau (Jin et al., 1999) and Namuco (0.6 g m^{-2} yr^{-1}) with an altitude between 4718 and 7111 m in the hinterlands of the Qinghai–Tibet Plateau (Wei et al., 2015). This is because Ruoergai has a lower altitude and continuous flooding (Chen et al., 2008; Hirota et al., 2004). Extrapolating the measurements at the eastern edge of the Tibetan Plateau to the whole plateau would inevitably result in estimation biases. The simulated average CH$_4$ flux from the Qinghai–Tibet Plateau in 1990 by CH4MOD$_{wetland}$ is 6.2 g m^{-1} yr^{-1} (5.0–7.2 g m^{-2} yr^{-1}), which is close to the observation at Huashixia and between the observations from Namucuo and Ruoergai.

Extrapolating measurements to the region can only be used to estimate the CH$_4$ emissions after the 1990s because measurement data were not available for earlier periods. Using the DLEM model, Xu and Tian (2012; Table 3) inferred a reduction of approximately 1.3 Tg CH$_4$ from Chinese marshlands between 1949 and 2008 due to marshland conversion and climate change. However, the study of Xu and Tian (2012) focused only on marshlands (natural wetlands excluding coastal wetlands, lakes, and rivers), which is equivalent to the inland wetlands in this study. However, our analysis showed that the coastal wetlands, lakes, and rivers represented approximately 40 % of the total wetland loss (Table 2) and thus are not negligible. The inclusion of the coastal wetlands, lakes, and rivers consolidates the estimation of the long-term changes in the CH$_4$ emissions from wetlands on regional/national scales.

Moreover, in northeastern China, the dominant vegetation is *Carex*. However, in Inner Mongolia, northwestern China, the North China Plain and the middle–lower Yangtze Plain, *Phragmites* represents the primary vegetation type (see Supplement S3). Although *Phragmites* usually has a larger biomass than *Carex*, the CH$_4$ fluxes are lower (according to a comparison between CH$_4$ fluxes in the perennial inland wetlands in ZL and SJ in Fig. S1; Table S1). If the observations of methane fluxes from the marshland dominated by *Carex* are used for the model calibration and used in the regions dominated by *Phragmites* (Xu and Tian, 2012), the national estimation might be overestimated. This is why the CH$_4$ reduction contributed 21.2 % in northwestern and northern China (including Region III and Region IV in this study) in the study of Xu and Tian (2012), while the contribution was only 7.3 % in this study.

4.2 Temporal variations in CH$_4$ emissions

Both the intra-annual and interannual CH$_4$ flux trends are largely influenced by the temperature and precipitation. The simulated seasonal variations in the CH$_4$ fluxes from the sites agreed with the observed values well (Fig. S1). The CH$_4$ flux and NPP peaked at the same time as the air temperature. The lowest CH$_4$ fluxes occurred during the winter or dry period, and the highest fluxes appeared during the summer and flooding period (Fig. S1). The intra-annual variations (Fig. 3) are similar to the simulated seasonal cycles in West Siberia (Bohn et al., 2015) or the Northern Hemisphere (Melton et al., 2013). The simulated fractions of CH$_4$ flux in the winter and freeze–thaw period in this study are similar to the observations of Yang et al. (2006).

Warming is expected to promote CH$_4$ fluxes from wetlands in the future (Zhuang et al., 2006; Christensen and Cox, 1995; Shindell et al., 2004). According to China's National Assessment Report on Climate Change (Ding and Ren, 2007), compared with the period 1961–1990, there will be a pronounced air temperature increase of 3.6–4.9 °C in the A2 and B2 scenarios (IPCC, 2000) by the end of this century in China. Based on our statistics, an increase of 3.6 °C would mean the national CH$_4$ flux increase ∼ 30 %. The air temperature is expected to increase more rapidly in northeastern China (Region I), northwestern China (Region III), and the North China Plain (the inland wetlands in Region IV; Ding and Ren, 2007), which indicates that there will be a larger promotion of CH$_4$ fluxes from the inland wetlands in these regions. For the Qinghai–Tibet Plateau (Region II), eastern China (the coastal wetlands in Region IV), and southern China (Region V), the climate-induced increase in CH$_4$ fluxes from inland and coastal wetlands will be lower.

The precipitation is expected to increase by 9–11 % by 2100, especially in northern China (Region I, Region III, and the inland wetlands in Region IV) and on the Qinghai–Tibet Plateau (Region IV; Ding and Ren, 2007). Based on the linear correlation analysis between the precipitation and CH$_4$ fluxes of the modeling results, an increase of 10 % (approximately 45 mm) would increase the national CH$_4$ fluxes by 0.8 g m^2 yr^{-1}.

Table 3. Estimation of CH_4 emissions from natural wetland in China.

Region	This study			Other studies			References
	CH_4 (Tg)	Period	Area (Mha)	CH_4 (Tg)	Period	Area (Mha)	
China[1]	3.0	1990	23.0	2.2	1988–2000	Nm	Wang et al. (1993)
China[1]	3.0	1990	23.0	1.7	1988	Nm	Khalil et al. (1993)
China[1]	3.0	1990	23.0	2.0	1996	18.7	Jin et al. (1999)
China[1]	3.0	1990	23.0	10.5	1990s	38.0	X. K. Wang et al. (2012)
China[1]	3.0	1990	23.0	6.65	1990	35.5	Cai (2012)
China[1]	2.2	2000	19.5	5.71	2000	30.5	Cai (2012)
China[1]	2.2	2000	19.5	3.15	2000	Nm	Chen et al. (2013)
China[1]	2.2	2000	19.5	4.76	2003–2009	9.0	Zhang et al. (2013)
China[2]	3.5	1950	20.3	3.2	1950	17.9	Xu and Tian (2012)
China[2]	2.7	1980	17.4	2.3	1980	13.0	Xu and Tian (2012)
China[2]	2.4	1990	13.5	2.0	1990	11.0	Xu and Tian (2012)
China[2]	1.6	2000	10.6	1.9	2000	9.4	Xu and Tian (2012)
China[2]	1.6	2010	10.0	1.9	2008	9.4	Xu and Tian (2012)
China[2]	1.6	2000	10.6	1.9	1995–2004	9.4	Tian et al. (2011)
China[2]	1.6	2000	10.6	1.8	1995–2004	9.4	Ding and Cai (2007)
NEC[2]	2.8	1950	12.3	2.2	1950	10.1	Xu and Tian (2012)
NEC[2]	1.2	2010	5.1	1.2	2008	4.7	Xu and Tian (2012)
NEC[2]	1.1	2000	5.4	1.2	2001–2002	2.8	Ding et al. (2004)
NEC[2]	1.1	2000	5.4	0.9	2000	Nm	Chen et al. (2013)
QTP[2]	0.3	1950	4.8	0.07	1950	0.8	Xu and Tian (2012)
QTP[2]	0.2	2008	3.2	0.06	2008	0.6	Xu and Tian (2012)
QTP[1]	0.45	1990	7.3	0.8	1996	3.5	Jin et al. (1999)
QTP[2]	0.23	2000	3.4	0.56	2001–2002	4.8	Ding et al. (2004)
QTP[2]	0.23	2000	3.4	1.25	2000	Nm	Chen et al. (2013)

[1] Natural wetland. [2] Natural wetland exclude coastal wetland, lakes, and rivers. Note: Nm, not mentioned in the literature; NEC, northeastern China; QTP, Qinghai–Tibet Plateau.

For the coastal wetlands, rising sea levels resulted from climate warming will reduce the area of coastal wetlands by inundation. Consider the Jiangsu Province in eastern China (Region IV) as an example, where 396, 617, and 1390 km^2 is expected to be lost in the next 30, 50, and 100 years, respectively (Li et al., 2006b). Moreover, rising sea levels will increase the invasion of salt water into estuarine wetlands (Shen et al., 2003; Hu et al., 2003; Huang and Xie, 2000), which will reduce CH_4 fluxes due to the higher salinity.

4.3 Present state and research gaps in CH_4 modeling

At this present time, there are still research gaps that need to be narrowed in simulating the national CH_4 emissions from natural wetlands by the improvement in process-based models.

The first improvement should focus on the flaws of model mechanism. Most of the existing process-based models, e.g., CH4MOD$_{wetland}$, CLM4Me (Riley et al., 2011), LPJ-WhyMe (Wania et al., 2010), DLEM (Tian et al., 2010, 2015; Xu et al., 2010), ORCHIDEE (Krinner et al., 2005), and SDGVM (Woodward et al., 1995; Beerling and Woodward, 2001), describe the process of CH_4 production, oxidation,

and transport processes in wetlands. In most of the models, the methane production rates are determined by the availability of methanogenic substrates and the influence of environmental factors. Most models use net primary production as an index to represent substrate availability for CH_4 production; thus they do not consider organic carbon in deep soils or in permafrost. In CH4MOD$_{wetland}$, the methanogenic substrates include root exudates, plant litter, and the soil carbon, which is a mechanism advantage over the DLEM, CLM4Me, and ORCHIDEE models. DLEM only considers CH_4 production from dissolved organic carbon (DOC). In CLM4Me, the CH_4 production is related to the heterotrophic respiration from soil and litter. ORCHIDEE uses a fraction of the most labile "litter + soil C" pool. Upon the methanogenic substrates, the influences of soil temperature, soil texture, and redox potential and PH are also incorporated in the models. However, the influence of soil salinity was usually ignored (e.g., CLM4Me, LPJ-WhyMe, DLEM, ORCHIDEE and SDGVM) or be simply processed (e.g., CH4MOD$_{wetland}$). The effect of thawing permafrost on the complex dynamics of hydrology and carbon substrates is now considered very important to the permafrost region (e.g., the Qinghai–Tibet Plateau).

At present, the parameterization related to the vegetation in wetlands was loosely constrained by the limited number of observations and the distribution of the plant species. The parameters in the CH$_4$ models usually refer to the production of labile organic compounds from gross primary production (GPP; e.g., f_{exu} in LPJ-WhyMe and VI in CH4MOD$_{wetland}$) and the CH$_4$ transportation and oxidation via plant aerenchyma (e.g., f_{oxid} in LPJ-WhyMe, P_{ox} in CH4MOD$_{wetland}$ and F_a in CLM4Me). These vegetation parameters are different among plant species but are usually unified in regional simulations. The differences in vegetation effectively influence the CH$_4$ fluxes as reported by King and Reeburgh (2002), documenting the relation between CH$_4$ and net primary production (NPP) in tundra vegetation. Verville et al. (1998) and Busch and Lösch (1999) have also shown the difference in the plant transport of CH$_4$ through aerenchymatous tissues between vegetation types. In this study, the herbaceous plant species other than *Carex* and *Phragmites* were not specifically considered. To reduce the uncertainty in estimating regional and national CH$_4$ emissions, the model parameterization concerning the wetland plants should receive more attention in modeling works.

The poor availability of the model inputs, especially the spatial variability in the water table depth, also accounts for a large proportion of the uncertainty in regional estimations. The TOPMODEL-based scheme (Beven and Kirkby, 1979) has been used to model regional water table depth in natural wetlands to drive the process-based models (Bohn et al., 2007; Kleinen et al., 2012; Lu and Zhuang et al., 2012; Zhu et al., 2013). It is based on the topographic wetness index (TWI) and assumes that water tables follow topographic holds (Haitjema and Mitchell-Bruker, 2005). However, the TWI is static and relies on the assumption that the local slope is an adequate proxy for the effective downslope hydraulic gradient, which is not necessarily true in low-relief terrains (Grabs et al., 2009). Therefore, this algorithm is less suitable in flat areas and will induce uncertainties in the simulated water table depth. Moreover, the HYDRO1k global values for the TWI provided by the USGS in 2000 (USGS, 2000) are the most commonly used data for the TOPMODEL method. However, the limited resolution and quality of the data can induce uncertainties, especially in tropical wetlands (Marthews et al., 2015; Collins et al., 2011). More accurate descriptions of the hydrology process and higher-resolution data sets are needed to reduce the error in the simulated water table depth.

Last but not least, the change in wetland area is a key factor that must be considered seriously. Unfortunately, time series data on wetland changes at regional scales are often unavailable. Popular methods for defining the extent of wetlands include using "prescribed constant wetland extents" and the "hydrological model" (Melton et al., 2013; Wania et al., 2013). Using different methods, Melton et al. (2013) reported that the estimate of global wetland area ranged from 7.1×10^6 to 26.9×10^6 km^2. The TOPMODEL scheme was extensively used to predict wetland distribution dynamics (Kleinen et al., 2012; Stocker et al., 2014; Melton et al., 2013). It is true that the hydrological model can reflect the annual or seasonal variations in the wetland area, which were considered to be the dominant cause of the seasonal variations in regional CH$_4$ emissions (Ringeval et al., 2010). However, this method is not suitable for simulating the historical wetland area in China. The reason is because the simulated wetland extent will not be sensitive to the influences of anthropogenic changes to the land surface (Wania et al., 2013), which could lead to an overestimate of the wetland area. In China, the annual marshland area had been temporally interpolated using a negative correlation between the Chinese population and the marshland area of 1950 and 2000 (Liu and Tian, 2010; Xu and Tian, 2012). However, this relationship inevitably resulted in large uncertainties because human activity was, though important, not the only driving factor in wetland changes (Niu et al., 2012). Furthermore, the influence of human disturbance should also be considered to improve the performance of the hydrological model (Melton et al., 2013; Wania et al., 2013) to more accurately delineate variations in the wetland extents at different temporal scales.

5 Projection of wetland changes in China and management tips

Restoration of wetlands has been one of the multiple measures in China to suppress environmental degradation. The national plan to establish wetland reserves of more than 1.4×10^9 ha in the China National Wetland Conservation Action Plan (NWCP) (Editorial Committee, 2009) will inevitably enhance methane emission to the atmosphere, as has been implied in the present study. However, if appropriate regional planning of the wetland restoration is implemented, less CH$_4$ will be emitted into the atmosphere. The rivers, lakes, and costal zones should be the first consideration for wetland restoration owing to the low methane fluxes. In the Qinghai–Tibet Plateau, the warming climate has resulted in melting of the permafrost soils and expansion of the lakes and rivers (Niu et al., 2012), in spite of the fact that higher temperature also stimulates evapotranspiration. In future, more attention will be paid to the conservation of the wetland biodiversity in the Qinghai–Tibet Plateau, because it can provide a variety of ecological functions and services. Northeastern China has become the most important food production region after wetland reclamation in the 1950s. The wetland there also has the highest CH$_4$ fluxes, as shown in the present study. Thus it is reasonable to keep the wetlands and croplands unchanged in this region and drain the wetland seasonally by proper management to mitigate the methane emissions. It is also worth noting that more and more artificial wetlands, e.g., wetland parks, are being established in urban areas of China to improve the living conditions of urban populations. The methane emission from the reclaimed-

water-flooded wetlands requires attention from further studies.

Author contributions. T. Li, W. Zhang, T. Vesala, and M. Raivonen designed the research; T. Li, Q. Zhang and G. Wang performed the CH$_4$ modeling; Y. Lu performed the TEM modeling; Z. Niu prepared the time series of the wetland area; and T. Li and W. Zhang prepared the manuscript with contribution from all coauthors.

References

An, S. Q., Li, H. B., Guan, B. H., Zhou, C. F., Wang, Z. S., Deng, Z. F., Zhi, Y. B., Liu, Y. L., Xu, C., Fang, S. B., Jiang, J. H., and Li, H. L.: China's natural wetlands: past problems, current status, and future challenges, Ambio, 36, 335–342, 2007.

Antonov, J. I., Seidov, D., Boyer, T. P., Locarnini, R. A., Mishonov, A. V., Garcia, H. E., Baranova, O. K., Zweng, M. M., and Johnson, D. R.: World Ocean Atlas 2009 Vol. 2, Salinity, in: NOAA Atlas NESDIS 69, edited by: Levitus, S., US Government Printing Office, Washington, D.C., 1–184, 2010.

Atkinson, L. P. and Hall, J. R.: Methane distribution and production in the Georgia salt marsh, Estuar. Coast. Mar. Sci., 4, 677–686, 1976.

Bartlett, K. B., Harriss, R. C., and Sebacher, D. I.: Methane flux from coastal salt marshes, J. Geophys. Res., 90, 5710–5720, 1985.

Bartlett, K. B., Bartlett, D. S., Harriss, R. C., and Sebacher, D. I.: Methane emissions along a salt marsh salinity gradient, Biogeochemistry, 4, 183–202, 1987.

Bastviken, D., Cole, J., Pace, M., and Tranvik, L.: Methane emissions from lakes: Dependence of lake characteristics, two regional assessments, and a global estimate, Global Biogeochem. Cy., 18, GB4009, doi:10.1029/2004GB002238, 2004.

Beerling, D. J. and Woodward, F. I.: Vegetation and the terrestrial carbon cycle: Modelling the first 400 Million Years, Cambridge University Press, Cambridge, 405 pp., 2001.

Belward, A. S., Estes, J. E., and Kline, K. D.: The IGBP-DIS global 1-km land-cover data set DISCover: A project overview, Photogramm. Eng. Rem. S., 65, 1013–1020, 1999.

Berrittella, C. and van Huissteden, J.: Uncertainties in modelling CH$_4$ emissions from northern wetlands in glacial climates: the role of vegetation parameters, Clim. Past, 7, 1075–1087, doi:10.5194/cp-7-1075-2011, 2011.

Beven, K. J. and Kirkby, M. J.: A physically based, variable contributing area model of basin hydrology, Hydrolog. Sci. Bull., 24, 43–69, 1979.

Bohn, T. J., Lettenmaier, D. P., Sathulur, K., Bowling, L. C., Podest, E., McDonald, K. C., and Friborg, T.: Methane emissions from western Siberian wetlands: heterogeneity and sensitivity to climate change, Environ. Res. Lett., 2, 045015, doi:10.1088/1748-9326/2/4/045015, 2007.

Bohn, T. J., Melton, J. R., Ito, A., Kleinen, T., Spahni, R., Stocker, B. D., Zhang, B., Zhu, X., Schroeder, R., Glagolev, M. V., Maksyutov, S., Brovkin, V., Chen, G., Denisov, S. N., Eliseev, A. V., Gallego-Sala, A., McDonald, K. C., Rawlins, M. A., Riley, W. J., Subin, Z. M., Tian, H., Zhuang, Q., and Kaplan, J. O.: WETCHIMP-WSL: intercomparison of wetland methane emissions models over West Siberia, Biogeosciences, 12, 3321–3349, doi:10.5194/bg-12-3321-2015, 2015.

Bousquet, P., Cialis, P., Miller, J. B., Dlugokencky, E. J., Hauglustaine, D. A., Prigent, C., van der Werf, G. R., Peylin, P., Brunke, E.-G., Carouge, C., Langenfelds, R. L., Lathière, J., Papa, F., Ramonet, M., Schmidt, M., Steele, L. P., Tyler, S. C., and White, J.: Contribution of anthropogenic and natural sources to atmospheric methane variability, Nature, 443, 439–443, doi:10.1038/nature05132, 2006.

Bush, J. and Lösch, R.: The Gas Exchange of Carex Species from Eutrophic Wetlands and its Dependence on Microclimatic and Soil Wetness Conditions, Phys. Chem. Earth B, 24, 117–120, 1999.

Cai, Z. C.: Greenhouse gas budget for terrestrial ecosystems in China, Sci. China Earth Sci., 55, 173–182, 2012.

Chen, H., Yao, S., Wu, N., Wang, Y., Luo, P., Tian, J., Gao, Y., and Sun, G.: Determinants influencing seasonal variations of methane emissions from alpine wetlands in Zoige Plateau and their implications, J. Geophys. Res., 113, D12303, doi:10.1029/2006JD008072, 2008.

Chen, H., Zhu, Q., Peng, C. H., Wu, N., Wang, Y. F., Fang, X. Q., Jiang, H., Xiang, W. H., Chang, X., Deng, X. W., and Yu G. R.: Methane emissions from rice paddies natural wetlands, lakes in China: synthesis new estimate, Glob. Change Biol., 19, 19–32, 2013.

Christensen, T. and Cox, P.: Response of methane emission from arctic tundra to climate change: results from a model simulation, Geophys. Res. Lett., 31, L04501, doi:10.1029/2003GL018680, 1995.

Christensen, T. R., Ekberg, A., Ström, L., Mastepanov, M., Panikov, N., Öquist, M., Svensson, B. H., Nykänen, H., Martikainen, P. J., and Oskarsson, H.: Factors controlling large scale variations in methane emissions from wetlands, Geophys. Res. Lett., 30, 1414, doi:10.1029/2002GL016848, 2003.

Collins, W. J., Bellouin, N., Doutriaux-Boucher, M., Gedney, N., Halloran, P., Hinton, T., Hughes, J., Jones, C. D., Joshi, M., Liddicoat, S., Martin, G., O'Connor, F., Rae, J., Senior, C., Sitch, S., Totterdell, I., Wiltshire, A., and Woodward, S.: Development and evaluation of an Earth-System model – HadGEM2, Geosci. Model Dev., 4, 1051–1075, doi:10.5194/gmd-4-1051-2011, 2011.

Cramer, W., Kicklighter, D. W., Bondeau, A., Moore Iii, B., Churkina, G., Nemry, B., Ruimy, A., Schloss, A. L., and The Participants of the Potsdam NPP Model Intercomparison: Comparing global models of terrestrial net primary productivity (NPP): overview and key results, Glob. Change Biol., 5, 1–15, 1999.

Davidson, N. C.: How much wetland has the world lost? Long-term and recent trends in global wetland area, Mar. Freshwater Res., 65, 934–941, 2014.

Denman, K. L., Brasseur, G., Chidthaisong, A., Ciais, P., Cox, P. M., Dickinson, R. E., Hauglustaine, D., Heinze, C., Holland, E., Jacob, D., Lohmann, U., Ramachandran, S., da Silva Dias, P. L., Wofsy, S. C., and Zhang, X.: Couplings between changes in the climate system and biogeochemistry, in: Climate Change 2007: The Physical Science Basis. Contribution of Working Group I to the Fourth Assessment Report of the Intergovernmanetal Panel on Climate Change, edited by: Solomon, S., Qin, D., Manning, M., Chen, Z., Marquis, M., Averyt, K. B., Tignor, M., and Miller, H. L., Cambridge University Press, Cambridge, 539–544, 2007.

Ding, W. X. and Cai, Z. C.: Methane emission from natural wetlands in China: summary of years 1995–2004 studies, Pedosphere, 17, 475–486, 2007.

Ding, Y. H. and Ren, G. Y.: Climate change in China and its future trend, in: National assessment report of climate change, edited by: editing committee of national assessment report of climate change, Science Press, China, 130–161, 2007 (in Chinese with English abstract).

Ding, W., X., Cai, Z., and Wang, D.: Preliminary budget of methane emissions from natural wetlands in China, Atmos. Environ., 38, 751–759, 2004.

Du, X. and Chen, W.: Methodology for managing the effect of uncertainty in simulation-based design, AIAA J., 38, 1471–1478, 2000.

Duan, X. N., Wang, X. K., Mu, Y. J., and Ouyang, Z. Y.: Seasonal and diurnal variations in methane emissions from Wuliangsu Lake in arid regions of China, Atmos. Environ., 39, 4479–4487, 2005.

Editorial Committee: China wetlands encyclopedia, Beijing Science and Technology Press, Beijing, 706 pp., 2009 (in Chinese).

Fan, Y. and van den Dool, H.: Climate prediction center global monthly soil moisture data set at 0.5° resolution for 1948 to present, J. Geophys. Res., 109, D10102, doi:10.1029/2003JD004345, 2004.

FAO/IIASA/ISRIC/ISS-CAS/JRC: Harmonized World Soil Database, version 1.0, FAO, Rome, Italy and IIASA, Laxenburg, Austria, 42 pp., 2008.

FAO/IIASA/ISRIC/ISSCAS/JRC: Harmonized World Soil Database, version 1.2, FAO and IIASA, Rome, Italy and Laxenburg, Austria, 43 pp., 2012.

Fung, I., John, J., Lerner, J., Matthews, E., Prather, M., Steele, L., and Fraser, P.: Three-dimensional model synthesis of the global methane cycle, J. Geophys. Res., 96, 13033–13065, 1991.

Gill, R. and Jackson, R. B.: Global Distribution of Root Turnover in Terrestrial Ecosystems, Oak Ridge National Laboratory Distributed Active Archive Center, Oak Ridge, Tennessee, USA, doi:10.3334/ORNLDAAC/661, 2003.

Giltrap, D. L., Li, C. C., and Saggar, S.: DNDC: A process-based model of greenhouse gas fluxes from agricultural soils, Agr. Ecosyst. Environ., 136, 292–300, 2010.

Grabs, T., Seibert, J., Bishop, K., and Laudon, H.: Modelling spatial patterns of saturated areas: A comparison of the topographic wetness index and a dynamic distributed model, J. Hydrol., 373, 15–23, 2009.

Haitjema, H. M. and Mitchell-Bruker, S.: Are water tables a subdued replica of the topography?, Ground Water, 43, 781–786, 2005.

Harris, I., Jones, P. D., Osborn, T. J., and Lister, D. H.: Updated high-resolution grids of monthly climatic observations-the CRU TS3.10 Dataset, Int. J. Climatol., 34, 623–642, doi:10.1002/joc.3711, 2014.

Hein, R., Crutzen, P. J., and Heimann, M.: An inverse modelling approach to investigate the global atmospheric methane cycle, Global Biogeochem. Cy., 11, 43–76, 1997.

Hirota, M., Tang, Y., Hu, Q., Hirata, S., Kato, T., Mo, W., Gao, G. M., and Marikoe, S.: Methane emissions from different vegetation zones in a Qinghai-Tibetan Plateau wetland, Soil Biol. Biochem., 36, 737–748, 2004.

Huang, G. H., Li, X. Z., Hu, Y. M., Shi, Y., and Xiao, D. N.: Methane emission from a natural wetland of northern China, J. Environ. Sci. Heal. A, 40, 1227–1238, 2005.

Huang, Y., Sun, W., Zhang, W., Yu, Y. Q., Su, Y. H., and Song, C. C.: Marshland conversion to cropland in northeast China from 1950 to 2000 reduced the greenhouse effect, Glob. Change Biol., 16, 680–695, 2010.

Huang, Z. G. and Xie, X. D.: Change of the sea level and its effect and countermeasures, Guangdong science and Technology Press, China, 263 pp., 2000 (in Chinese).

Hu, S., Zhu, J. R., Fu, D. J., and Wu, H.: Estuarine circulation and saltwater intrusion II: impacts of river discharge and rise of sea level, Journal of Ocean University of Qingdao, 33, 337–342, 2003 (in Chinese with English abstract).

IPCC: Emission Scenarios: A Special Report of Workgroup III of IPCC, Cambridge University Press, UK, 78 pp., 2000.

IPCC: Climate Change 2013: The Physical Science Basis. Contribution of Working Group I to the Fifth Assessment Report of the Intergovernmental Panel on Climate Change, edited by: Stocker, T. F., Qin, D., Plattner, G. K., Tignor, M., Allen, S. K., Boschung, J., Nauels, A., Xia, Y., Bex, V., and Midgley, P. M., Cambridge University Press, Cambridge, 52–53, 2013.

Jin, H. J., Wu, J., Cheng, G. D., Tomoko, N., and Sun, G. Y.: Methane emissions from wetlands on the Qinghai-Tibet Plateau, Chinese Sci. Bull., 44, 2282–2286, 1999.

Kesik, M., Ambus, P., Baritz, R., Brüggemann, N., Butterbach-Bahl, K., Damm, M., Duyzer, J., Horváth, L., Kiese, R., Kitzler, B., Leip, A., Li, C., Pihlatie, M., Pilegaard, K., Seufert, S., Simpson, D., Skiba, U., Smiatek, G., Vesala, T., and Zechmeister-Boltenstern, S.: Inventories of N$_2$O and NO emissions from European forest soils, Biogeosciences, 2, 353–375, doi:10.5194/bg-2-353-2005, 2005.

Khalil, M. A. K., Shearer, M. J., and Rasmussen, R. A.: Methane sources in China: historical and current emissions, Chemosphere, 26, 127–142, 1993.

King, G. M. and Wiebe, W. J.: Methane release from soils of a Georgia salt marsh, Geochim. Cosmochim. Ac., 42, 343–348, 1978.

King, J. Y. and Reeburgh, W. S.: A pulse-labeling experiment to determine the contribution of recent plant photosynthates to net methane emission in arctic wet sedge tundra, Soil Biol. Biochem., 34, 173–180, 2002.

Kleinen, T., Brovkin, V., and Schuldt, R. J.: A dynamic model of wetland extent and peat accumulation: results for the Holocene, Biogeosciences, 9, 235–248, doi:10.5194/bg-9-235-2012, 2012.

Krinner, G., Viovy, N., de Noblet-Ducoudre, N., Ogee, J., Polcher, J., Friedlingstein, P., Ciais, P., Sitch, S., and Prentice, I. C.: A dynamic global vegetation model for studies of the coupled atmosphere-biosphere system, Global Biogeochem. Cy., 19, 941–962, 2005.

Lang, H. Q. and Zu, W. C.: Marshland in Chinese, Shandong Science and Technology Press, China, 269 pp., 1983 (in Chinese).

Li, C. C., Narayanan, V., and Harriss, R. C.: Model estimates of nitrous oxide emissions from agricultural lands in the United States, Global Biogeochem. Cy., 10, 297–306, 1996.

Li, C. C., Arvin, M., Reiner, W., Cai, Z. C., Zheng, X. H., Huang, Y., Haruo, T., Jariya, B., and Rhoda, L.: Modelling greenhouse gas emissions from rice production systems: Sensitivity and upscaling, Global Biogeochem. Cy., 18, GB1043, doi:10.1029/2003GB002045, 2004.

Li, C., Salas, W., DeAngelo, B., and Rose, S.: Assessing alternatives for mitigating net greenhouse gas emissions and increasing yields from rice production in China over the next twenty years, J. Environ. Qual., 35, 1554–1565, 2006a.

Li, J. L., Wang, Y. H., Zhang, R. S., Qi, D. L. and Zhang, D. F.: Disaster effects of sea level rise – a case of Jiangsu coastal low land, Sci. Geograph. Sinica, 26, 87–93, 2006b (in Chinese with English abstract).

Li, T., Huang, Y., Zhang, W., and Song, C.: CH4MOD$_{wetland}$: A biogeophysical model for simulating CH$_4$ emissions from natural wetland, Ecol. Model., 221, 666–680, 2010.

Li, T., Huang, Y., Zhang, W., and Yu, Y.-Q.: Methane emissions associated with the conversion of marshland to cropland and climate change on the Sanjiang Plain of northeast China from 1950 to 2100, Biogeosciences, 9, 5199–5215, doi:10.5194/bg-9-5199-2012, 2012.

Liu, M. and Tian, H.: China's land cover and land use change from 1700 to 2005: Estimations from high-resolution satellite data and historical archives, Global Biogeochem. Cy., 24, GB3003, doi:10.1029/2009GB003687, 2010.

Loveland, T. R., Brown, J. F., Ohlen, D. O., Zhu, Z., Yang, L., Merchant, J. W., and Reed, B. C.: Development of a global land cover characteristics database and IGBP DISCover from 1 km AVHRR data, Int. J. Remote Sens., 21, 1303–1330, 2000.

Lu, X. and Zhuang, Q.: Modelling methane emissions from the Alaskan Yukon River basin, 1986-2005, by coupling a larg-scale hydrological model and a process-based methane model, J. Geophys. Res., 117, G02010, doi:10.1029/2011JG001843, 2012.

Magenheimer, J. F., Moore, T. R., Chmura, G. L., and Daoust, R. J.: Methane and carbon dioxide flux from a macrotidal salt marsh, Bay of Fundy, New Brunswick Canada, Estuaries, 19, 139–145, 1996.

Marthews, T. R., Dadson, S. J., Lehner, B., Abele, S., and Gedney, N.: High-resolution global topographic index values for use in large-scale hydrological modelling, Hydrol. Earth Syst. Sci., 19, 91–104, doi:10.5194/hess-19-91-2015, 2015.

McGuire, A. D., Melillo, J. M., Joyce, L. A., Kicklighter, D. W., Grace, A. L., Moore III, B., and Vorosmarty, C. J.: Interactions between carbon and nitrogen dynamics in estimating net primary productivity for potential vegetation in North America, Global Biogeochem. Cy., 6, 101–124, 1992.

Melillo, J. M., Mcguire, A. D., Kicklighter, D. W., Moore, B., Vorosmarty, C. J., and Schloss, A. L.: Global climate change and terrestrial net primary production, Nature, 363, 234–240, 1993.

Melton, J. R., Wania, R., Hodson, E. L., Poulter, B., Ringeval, B., Spahni, R., Bohn, T., Avis, C. A., Beerling, D. J., Chen, G., Eliseev, A. V., Denisov, S. N., Hopcroft, P. O., Lettenmaier, D. P., Riley, W. J., Singarayer, J. S., Subin, Z. M., Tian, H., Zürcher, S., Brovkin, V., van Bodegom, P. M., Kleinen, T., Yu, Z. C., and Kaplan, J. O.: Present state of global wetland extent and wetland methane modelling: conclusions from a model intercomparison project (WETCHIMP), Biogeosciences, 10, 753–788, doi:10.5194/bg-10-753-2013, 2013.

Montzka, S. A., Dlugokencky, E. J., and Butler, J. H.: Non-CO$_2$ greenhouse gases and climate change, Nature, 476, 43–50, 2011.

Moser, M., Prentice, C., and Frazier, S.: A global overview of wetland loss and degradation. Proceedings to the 6th Meeting of the Conference of Contracting Parties of the Ramsar Convention, Brisbane, Australia, Vol. 10/12B, 21–31, March 1996.

Nisbet, E. G., Dlugokencky, E. J., and Bousquet, P.: Methane on the rise-again, Science, 343, 493–495, 2014.

Niu, Z. G., Zhang, H. Y., Wang, X. W., Yao W. B., Zhou, D. M., Zhao, K. Y., Zhao, H., Li, N. N., Huang, H. B., Li, C. C., Yang, J., Liu, C. X., Liu, S., Wang, L., Li, Z., Yang, Z. Z., Qiao, F., Zheng, Y. M., Chen, Y. L., Sheng, Y. W., Gao X. H., Zhu, W. H., Wang, W. Q., Wang, H., Weng, Y. L., Zhuang, D. F., Liu, J. Y., Luo, Z. C., Cheng, X., Guo, Z. Q., and Gong, P.: Mapping wetland changes in China between 1978 and 2008, Chinese Sci. Bull., 57, 2813–2823, 2012.

Poffenbarger, H. J., Needelman, B. A., and Megonigal, J. P.: Salinity influence on methane emissions from tidal marshes, Wetlands, 31, 831–842, 2011.

Potter, C., Klooster, S., Hiatt, S., Fladeland, M., Genovese, V., and Gross, P.: Methane emissions from natural wetlands in the United States: satellite-derived estimation based on ecosystem carbon cycling, Earth Interact., 10, 1–12, 2006.

Revenga, C., Brunner, J., Henninger, N., Kassem, K., and Payne, R.: Pilot analysis of global ecosystems: Freshwater systems, World Resources Institute, Washington, DC, 78 pp., 2000.

Riley, W. J., Subin, Z. M., Lawrence, D. M., Swenson, S. C., Torn, M. S., Meng, L., Mahowald, N. M., and Hess, P.: Barriers to predicting changes in global terrestrial methane fluxes: analyses using CLM4Me, a methane biogeochemistry model integrated in CESM, Biogeosciences, 8, 1925–1953, doi:10.5194/bg-8-1925-2011, 2011.

Ringeval, B., de Noblet, N., Ciais, P., Bousquet, P., Prigent, C., Papa, F., and Rossow, W. B.: An attempt to quantify the impact of changes in wetland extent on methane emissions on the seasonal and interannual time scales, Global Biogeochem. Cy., 24, GB2003, doi:10.1029/2008GB003354, 2010.

Shen, H. T., Mao, Z. C., and Zhu, J. R.: Salt water intrusion in ChangJiang Estuary, China Ocean Press, China, 175 pp., 2003 (in Chinese with English abstract).

Shindell, D. T., Walter, B. P., and Faluvegi, G.: Impacts of climate change on methane emissions from wetlands, Geophys. Res. Lett., 31, L21202, doi:10.1029/2004GL021009, 2004.

Song, C. C., Zhang, J. B., Wang, Y. Y., Wang, Y. S., and Zhao, Z. C.: Emission of CO$_2$, CH$_4$ and N$_2$O from freshwater marsh in northeast of China, J. Environ. Manage., 40, 6879–6885, 2007.

Stocker, B. D., Spahni, R., and Joos, F.: DYPTOP: a cost-efficient TOPMODEL implementation to simulate sub-grid spatio-temporal dynamics of global wetlands and peatlands, Geosci. Model Dev., 7, 3089–3110, doi:10.5194/gmd-7-3089-2014, 2014.

Streets, D. G., Jiang, K., Hu, X., Sinton, J. E., Zhang, X.-Q., Xu, D., Jacobson, M. Z., and Hansen, J. E.: Recent reductions in China's greenhouse gas emissions, Science, 294, 1835–1837, 2001.

Tian, H., Xu, X., Liu, M., Ren, W., Zhang, C., Chen, G., and Lu, C.: Spatial and temporal patterns of CH$_4$ and N$_2$O fluxes in terrestrial ecosystems of North America during 1979–2008: application of a global biogeochemistry model, Biogeosciences, 7, 2673–2694, doi:10.5194/bg-7-2673-2010, 2010.

Tian, H., Xu, X., Lu, C., Liu, M. L., Ren, W., Chen, G. S., Melillo, J., and Liu, J. Y.: Net exchanges of CO$_2$, CH$_4$, and N$_2$O between China's terrestrial ecosystems and the atmosphere and their contributions to global climate warming, J. Geophys. Res., 116, G02011, doi:10.1029/2010JG001393, 2011.

USGS: US Geological Survey: HYDRO1k Elevation derivative database, US Geological Survey Earth Resources Observation and Science (EROS) Center, Sioux Falls, South Dakota, https://lta.cr.usgs.gov/HYDRO1KReadMe (last access: 26 November 2015), 2000.

Verville, J. H., Hobbie, S. E., Chapin III, F. S., and Hooper, D. U.: Response of tundra CH$_4$ and CO$_2$ flux to manipulation of temperature and vegetation, Biogeochemistry, 41, 215–235, 1998.

Wang, M. X., Dai, A. G., Huang, J., Ren, L. X., and Shen, R. X.: Sources of methane in China: rice fields, agricultural waste treatment, cattle, coal mines, and other minor sources, Scientia Atmospherica Sinica, 17, 52–64, 1993 (in Chinese with English abstract).

Wang, Z., Wu, J., Madden, M., and Mao, D.: China's wetlands: conservation plans and policy impacts, Ambio, 41, 782–786, 2012.

Wang, X. K., Lu, F., and Yang, L.: Methane emissions from China's natural wetlands: measurements, temporal variations and influencing factors, in: Recarbonization of the Biosphere, edited by: Lal, R., Lorenz, K., Hüttl, R. F., Schneider, B. U., and von Braun, J., Springer Netherlands, 99–125, 2012.

Wania, R., Ross, I., and Prentice, I. C.: Implementation and evaluation of a new methane model within a dynamic global vegetation model: LPJ-WHyMe v1.3.1, Geosci. Model Dev., 3, 565–584, doi:10.5194/gmd-3-565-2010, 2010.

Wania, R., Melton, J. R., Hodson, E. L., Poulter, B., Ringeval, B., Spahni, R., Bohn, T., Avis, C. A., Chen, G., Eliseev, A. V., Hopcroft, P. O., Riley, W. J., Subin, Z. M., Tian, H., van Bodegom, P. M., Kleinen, T., Yu, Z. C., Singarayer, J. S., Zürcher, S., Lettenmaier, D. P., Beerling, D. J., Denisov, S. N., Prigent, C., Papa, F., and Kaplan, J. O.: Present state of global wetland extent and wetland methane modelling: methodology of a model inter-comparison project (WETCHIMP), Geosci. Model Dev., 6, 617–641, doi:10.5194/gmd-6-617-2013, 2013.

Wei, D., Xu, R., Tenzin, T., Dai, D. X., Wang, Y. S., and Wang, Y. H.: Revisiting the role of CH$_4$ emissions from alpine wetlands on the Tibetan Plateau: evidence from two in situ measurements at 4758 and 4320 m above sea level. J. Geophys. Res.-Biogeo., 120, 1471001450, doi:10.1002/2015JG002974, 2015.

Whalen, S. C.: Biogeochemistry of methane exchange between natural wetlands and the atmosphere, Environ. Eng. Sci., 22, 73–94, 2005.

Woodward, F. I., Smith, T. M., and Emanuel, W. R.: A global land primary productivity and phytogeography model, Global Biogeochem. Cy., 9, 471–490, 1995.

Xu, Q., Cai, L., and Dong, Y. H.: Characteristics, types and management of the wetlands in China: Study on wetlands in China, edited by Chen Y. Y., Jilin Science and Technology Press, Changchun, Jilin, China, 24–33, 1995 (in Chinese).

Xu, X. F., Tian, H. Q., Zhang, C., Liu, M. L., Ren, W., Chen, G. S., Lu, C. Q., and Bruhwiler, L.: Attribution of spatial and temporal variations in terrestrial methane flux over North America, Biogeosciences, 7, 3637–3655, doi:10.5194/bg-7-3637-2010, 2010.

Xu, X. and Tian, H.: Methane exchange between marshland and the atmosphere over China during 1949–2008, Global Biogeochem. Cy., 26, GB2006, doi:10.1029/2010GB003946, 2012.

Yan, X., Akiyama, H., Yagi, K., and Akimoto, H.: Global estimations of the inventory and mitigation potential of methane emissions from rice cultivation conducted using the 2006 Intergovernmental Panel on Climate Change Guidelines, Global Biogeochem. Cy., 23, GB2002, doi:10.1029/2008GB003299, 2009.

Yang, W. Y., Song, C. C., and Zhang, J. B.: Dynamics of methane emissions from a freshwater marsh of northeast China, Sci. Total Environ., 371, 286–292, 2006.

Yang, H., Xie, P., Ni, L., and Flower, R. J.: Underestimation of CH$_4$ emission from freshwater lakes in China, Environ. Sci. Technol., 45, 4203–4204, 2011.

Zhang, W., Yu, Y., Huang, Y., Li, T., and Wang, P.: Modelling methane emissions from irrigated cultivation in China from 1960 to 2050, Glob. Change Biol., 17, 3511–3523, 2011.

Zhang, X., Jiang, H., Lu, X., Cheng, M., Zhang, X., Li, X., and Zhang, L.: Estimate of methane release from temperate natural wetlands using ENVISAT/SCIAMACHY data in China, Atmos. Environ., 69, 191–197, 2013.

Zhao, K. Y.: Mires in China, Science Press, Beijing, China, 1999 (in Chinese).

Zhao, K. Y. and Liu, X. T.: Status qua and prospect of studies in wetlands, Study on wetlands in China, Jilin Science and Technology Press, Changchun, Jilin, China, 1–9, 1995 (in Chinese).

Zhu, X. D., Zhuang, Q. L., Xiang, G., Sokolov, A., and Schlosser, C. A.: Pan-Arctic land-atmospheric fluxes of methane and carbon dioxide in response to climate change over the 21st century, Environ. Res. Lett., 8, 045003, doi:10.1088/1748-9326/8/4/045003, 2013.

Zhuang, Q., Melillo, J., Kicklighter, D., Prinn, R. G., McGuire, A. D., Steudler, P. A., Felzer, B. S., and Hu, S.: Methane fluxes between terrestrial ecosystems and the atmosphere at northern high latitudes during the past century: A retrospective analysis with a process-based biogeochemistry model, Global Biogeochem. Cy., 18, GB3010, doi:10.1029/2004GB002239, 2004.

Zhuang, Q., Mellillo, J., Sarofim, M., Kicklighter, D. W., McGuire, A. D., Felzer, B. S., Sokolov, A., Prinn, R. G., Steudler, P. A., and Hu, S: CO$_2$ and CH$_4$ exchanges between land ecosystems and the atmosphere in northern high latitudes over the 21st century, Geophys. Res. Lett., 33, L17403, doi:10.1029/2006GL026972, 2006.

Zhuang, Q., Melillo, J., Mcguire, A., Kicklighter, D., Prinn, R. G., Steudler, P. A., Felzer, B. S., and Hu, S.: Net emissions of CH$_4$ and CO$_2$ in Alaska: Implications for the region's greenhouse gas budget, Ecolog. Appl., 17, 203–212, 2007.

Zhuang, Q., Chen, M., Xu, K., Tang, J., Saikawa, E., Lu, Y., Melillo, J. M., Prinn, R. G., and McGuire, A. D.: Response of global soil consumption of atmospheric methane to changes in atmospheric climate and Nitrogen deposition, Global Biogeochem. Cy., 27, 650–663, 2013.